Beyond Conventional Migration - Nonlinear Subsalt Imaging with Transmissions and Two-sided Illumination

Amsterdam '14

Th G103 04

Beyond Conventional Migration - Nonlinear Subsalt Imaging with Transmissions and Two-sided Illumination

M. Ravasi (University of Edinburgh), I. Vasconcelos* (Schlumberger Gould Research) & A. Curtis (University of Edinburgh)

SUMMARY

Conventional (linear) migration algorithms use only a small portion of recorded seismic data (primary reflections) because they rely on single-scattering assumptions. Nonlinear imaging methods also use reflected multiply-scattered waves, benefiting from their additional illumination and sensitivity to the model. Primary and multiple reflections are, however, just part of the energy generated during a seismic experiment - transmitted waves are also generated but are usually not recorded by one-sided (surface seismic) acquisition systems. In theory only two-sided illumination of the imaging target would allow this energy to be recorded and used in migration. Here we use a synthetic example of subsalt imaging to show the nature of improvements to the seismic image (and extended image) from the use of multiples and transmitted waves. We then suggest a practical approach to construct the additional fields required by nonlinear two-sided imaging without the need of a velocity model with sharp contrasts and receivers (and/or sources) in the subsurface.

Introduction

Reverse-time migration (RTM) is now a standard industrial imaging technique, usually preferred over other migration methods for imaging complex geologies. Conventional RTM relies on the first-order Born approximation (e.g., Stolt and Weglein, 1985), and thus accurately accounts for only the linear or single-scattered portion of the seismic data (Biondi, 2006), failing to properly migrate multiply scattered events. Nonlinear imaging methods (Halliday and Curtis, 2010; Fleury and Vasconcelos, 2012; Vasconcelos, 2013; Fleury, 2013; Ravasi and Curtis, 2013) additionally use nonlinear, multiply-scattered events to reduce image artifacts and sharpen contrasts in the image. However, even when including nonlinearities, the lack of enclosing boundaries (using one-sided surface seismic illumination) represents another challenge to the practice of seismic imaging: limited source and receiver aperture is known to cause image distortions.

We use a synthetic subsalt imaging experiment to study the advantages of incorporating nonlinear interactions and two-sided acquisition in terms of increasing illumination and resolution of the seismic image. We then discuss a practical approach to construct the required fields for nonlinear two-sided imaging without relying on knowledge of the detailed structure of the correct model (e.g., sharp impedance contrasts), and having receivers and/or sources at depth.

Linear and nonlinear migration

Wave-equation imaging consists of two steps: first numerical modelling to extrapolate source w_{src} and receiver w_{rec} wavefields from source and receiver positions into the subsurface, and second the application of an imaging condition to create the image i. Conventional linear RTM generates the required wavefields via an estimated (smooth) reference model and the recorded scattered data (d_S), and a correlation imaging condition is applied

$$w^{l}_{S,rec} = \int_{\partial V_r} d_S G^{*}_0 d\mathbf{x}_r \qquad\qquad i^{l} = \int_{\partial V_r} w^{*}_{0,src} w^{l}_{S,rec} d\mathbf{x}_s \tag{1}$$

where $w^{l}_{\mathrm{S,rec}}$ is the linear scattered receiver wavefield and $w_{0,\mathrm{src}}$ is the reference source wavefield. G_0 is the receiver-side reference propagator and * represents complex conjugation resulting in crosscorrelation in the frequency domain. Integration is carried out along the available boundaries of receivers ∂V_r and sources ∂V_s: in this work, when $\partial V_r = \partial V_{r,top}$, $\partial V_s = \partial V_{s,top}$ we will refer to one-sided illumination, while two-sided illumination is given by $\partial V_r = \partial V_{r,top} \cup \partial V_{r,bot}$, as in Figure 1.

Nonlinear RTM (e.g., Vasconcelos, 2013) goes beyond the single-scattering assumption and focuses also the contribution of multiply scattered waves. The wavefield extrapolation step is modified to account for nonlinearities arising at the receiver-side (waves that interact multiple times with model perturbations on the path from the imaging point to the recording surface). The recorded full data (d) is back-propagated using the receiver-side scattered/total propagator G_S / G as in

$$w^{nl}_{S,rec} = w^{l}_{S,rec} + \int_{\partial V_r} dG^{*}_S d\mathbf{x}_r, \quad w^{nl}_{rec} = \int_{\partial V_r} dG^{*} d\mathbf{x}_r \tag{2}$$

to construct the nonlinear scattered receiver wavefield $w^{nl}_{\mathrm{S,rec}}$ and hence the nonlinear total receiver wavefield w^{nl}_{rec} (by adding the reference field G_0). A second term is also added to the imaging condition (Fleury and Vasconcelos, 2012) to account for source-side nonlinearities:

$$i^{nl} = \int_{\partial V_r} w^{*}_{0,src} w^{nl}_{S,rec} d\mathbf{x}_s + \int_{\partial V_r} w^{*}_{S,src} w^{nl}_{rec} d\mathbf{x}_s \tag{3}$$

where $w_{S,src}$ is the scattered source wavefield.

Example

Our example uses a modified version of the synthetic dataset Pluto 1.5 released by the SMAART JV consortium, with a flat seabed at a depth of $z_{sb,top}=760\ m$ and a second water layer added at the bottom of the model ($z_{sb,bot}=7{,}600\ m$) to model a symmetrical lower acquisition surface of receivers (Figure 1a). The synthetic data are modeled using 51 sources placed at 40m depth, two fixed arrays of receivers along the upper and lower seabeds, a Ricker wavelet pulse with 15-Hz peak frequency, and absorbing boundaries (i.e., in the absence of a free-surface). Four different imaging experiments are performed, differing in terms of illumination (one- or two-sided) and type of migrated events (single or multiple scattering) (Figure 1b-e). The imaging outputs (i.e., images and extended images) are

compared in terms of resolution, illumination, and presence of cross-talk noise, giving special attention to areas just above and below the salt body on the right where illumination (below) and cross-talk (above) issues are usually severe.

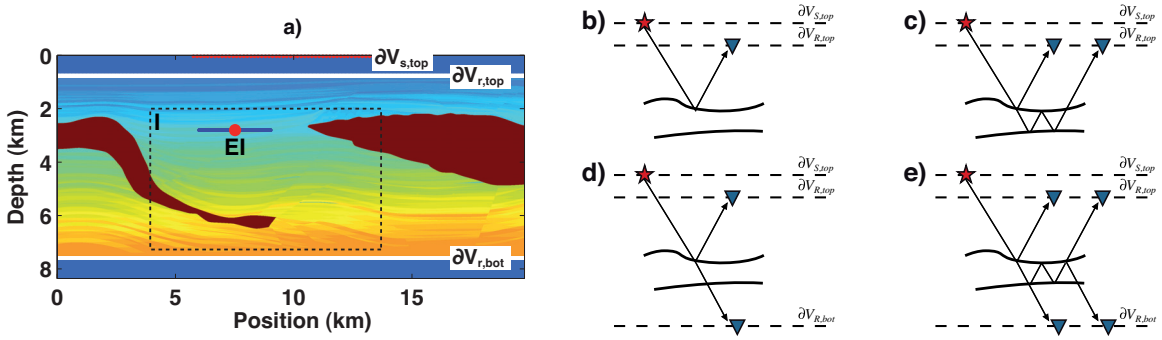

Figure 1 *(a) Pluto model along with shot locations (red dots), receiver geometry (white lines), and extended image survey "EI". (b-e) Schematic representations of four different imaging experiments carried out: (b) one-sided linear RTM, (c) two-sided linear RTM, (d) one-sided nonlinear RTM, and (e) two-sided nonlinear RTM. Images are computed inside the windowed area "I".*

Images - Figure 2a shows the conventional image obtained by means of one-sided linear RTM, performed using a smoothed version of the model in Figure 1 but keeping sharp boundaries at the fluid-solid interfaces and at the edges of the salt bodies. The structure is clear only in the shallow part, while illumination issues are present below the two salt bodies since such portions of the model are poorly illuminated by primaries. One-sided nonlinear RTM, is displayed in Figure 2b. The uplift arising from the additional focusing of nonlinear multiple-scattered energy (e.g., internal multiples) at any image point is remarkable: interfaces are more clearly defined also in the deeper section, there is a general increase in the spatial resolution of the image structure (see, for example, the resolution of the faults), and areas that are poorly illuminated by single-scattering events are better resolved. The artifacts affecting the top of the salt body on the right are also significantly suppressed and the nonlinear image in Figure 2b reveals the complex structure showing again the power of focussing multiples together with primaries. The value of having a second boundary of receivers at the bottom of the model is shown in Figure 2c and 2d. Transmitted waves are shown to contain useful additional information that is responsible for a more accurate imaging below salt bodies (high-impedance obstructions). Illumination of the imaging target from different directions equalizes the amplitudes in two-sided images and compensates for cross-talk (spurious) artifacts arising in the images when one-sided data are migrated.

Extended images - We construct an extended image (Vasconcelos *et al.*, 2010) at a depth of z_{EI} = 2,800 m. Figure 3 compares the directly modeled extended image (Figure 3a) with those obtained from the four experiments in Figure 1. From the one-sided RTM EI (Figure 3b) we notice how upgoing events (i.e., blue arrows), such as reflections coming from the top of the salt on the left and the bottom seabed, are generally reconstructed in the causal part, while downgoing events (i.e., red arrows) are constructed in the acausal panel. Adding the nonlinear terms to the extended image (Figure 3c) is beneficial in a number of ways: first, multiples are successfully turned into physical events by means of scattered propagators which add energy to those obtained by conventional imaging (e.g., the change in amplitudes of the event at 3.5s in Figure 3b and 3c). Second, multiples provide non-physical contributions that totally (or partially) annul those arising in RTM. As a result, the energy mapped around zero-offset and zero-time is better focused for nonlinear RTM than for RTM (see close-ups in Figure 3b and 3c); this feature is directly linked to the overall improvement in resolution of nonlinear over conventional linear imaging (Vasconcelos, 2013). The advantage of also having receivers below the imaging target can be appreciated by inspection of two-sided RTM (Figure 3d) and nonlinear RTM (Figure 3e) extended images. Transmitted data from top sources are mainly responsible for constructing upgoing waves in the acausal panel and downgoing waves in the causal panel. It is important to observe that causal and acausal panels become very similar in terms of event construction and amplitudes when all the contributions are summed together (Figure 3e). Since the final EI should converge to the homogenous (time-symmetric) Green's function, time symmetry in the gather around $t = 0s$ constitutes a means to assess the quality of the extended images.

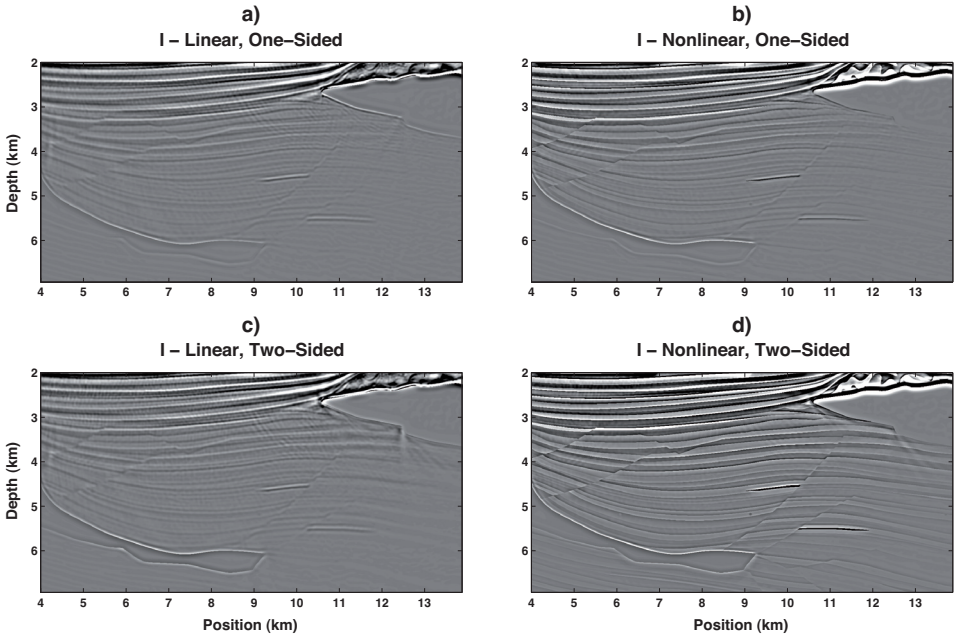

Figure 2 *Images obtained by means of (a) linear and (b) nonlinear RTM using sources and receivers only above the imaging target. Similarly, (c) and (d) are the two-sided linear and nonlinear images.*

Two-sided nonlinear imaging: a practical approach

The availability of only a (relatively smooth) reference background velocity model at the imaging stage has led most imaging algorithms to rely on a linearising, single-scattering assumption (Biondi, 2006), by neglecting complex scattering effects. To overcome this limitation, an accurate knowledge of the full wavefield propagating from any point in the subsurface to the receiver array is required to downward continue multiple reflections/diffractions traveling from that subsurface point to the recording surface, as shown in equations 2. Similarly, an estimate of the full wavefield from the source array to any subsurface point (equation 3) allows waves that bounce multiple times in their path from the source to the subsurface point to be properly imaged.

Although here we have assumed exact knowledge of the wavefield propagators, one practical way to account for multiples in the propagators may be represented by the *autofocusing* technique proposed by Broggini *et al.* (2012) and Wapenaar *et al.* (2013). These authors show that it is possible to estimate the correct Green's function including all internal multiples from a virtual source anywhere inside the medium given only the measured reflection data and an estimate of the direct arrival from the virtual source to the recording surface. This also provides the response observed by a virtual receiver in the subsurface from sources at the surface by using a source-receiver reciprocity argument. Thus we obtain the full (source- and receiver-side) propagators required by the nonlinear terms in both the wavefield extrapolation and imaging conditions above. Similarly, given a one-sided acquisition setup, the autofocusing method also can be tailored to reconstruct (and then migrate) transmission data. Responses from virtual sources selected at an arbitrarily depth level to the recording surface can be reconstructed, and the same source-receiver reciprocity argument can be invoked to obtain a virtual array of receivers at depth. This method has only been proven for acoustic waves, and a first extension to elastic data is in da Costa *et al*. (2014). However, it has not been tested on real data, and hence practical limitations have yet to be addressed.

Conclusions

Conventional reverse-time migration is known to produce images that exhibit acquisition imprints and poorly illuminated areas, especially in highly complex subsurface environments. We have shown that exploiting multiple reflections in the imaging process with the correct full or scattered source and receiver propagators mitigates these problems and increases the resolution of the migrated image because multiples provide better subsurface illumination. Imaging with two-sided acquisition geometries makes use of information contained in the transmitted component of recorded wavefields

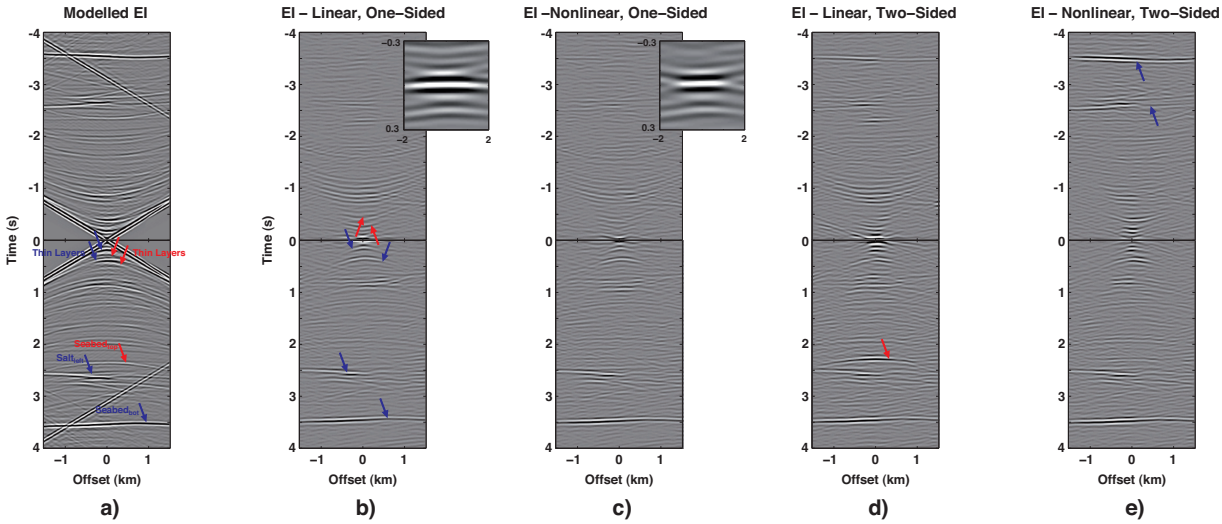

Figure 3 *Extended images constructed via (a) direct modeling, (b) one-sided RTM, (c) one-sided nonlinear RTM, (d) two-sided RTM, and (e) two-sided nonlinear RTM. Close-ups show focusing around zero-offset zero-time for one-sided migration, while blue/red arrows identify up/downgoing reconstructed energy in the different experiments.*

responsible for the construction of some (not all) of the events: upgoing events are mainly constructed in the causal part while downgoing events are in the acausal one. Multiple reflections, properly handled via nonlinear imaging, provide additional contributions to some of the physical events given by linear imaging and sometimes also correct their polarity; transmissions construct events that are complementary to those from reflection data (e.g., transmission data construct upgoing waves in the acausal part and downgoing waves in the causal part), improving the time symmetry in reconstructed gathers.

Acknowledgements

The authors thank the Edinburgh Interferometry Project (EIP) sponsors (ConocoPhillips, Schlumberger, Statoil, and Total) for supporting this research. We are thankful to James Rickett and Dirk-Jan van Manen for insightful discussions and inputs. This work was performed while Matteo Ravasi was an intern at Schlumberger Gould Research.

References

Biondi, B. [2006] 3D seismic imaging. SEG.

Broggini, F., Snieder, R., and Wapenaar, K. [2012] Focusing the wavefield inside an unknown 1D medium – beyond seismic interferometry. Geophysics, **77**, (5), A25-A28.

da Costa, C., Ravasi, M., Meles, G., and Curtis, A. [2014] Elastic autofocusing. 76th EAGE Conference & Exhibition Extended Abstracts.

Fleury, C. [2013] Increasing illumination and sensitivity of reverse-time migration with internal multiples. Geophysical Prospection, **61**, (5), 891-906.

Fleury, C. and Vasconcelos, I., [2012] Imaging condition for nonlinear scattering-based imaging: Estimate of power loss in scattering. Geophysics, **77**, (1), S1-S18.

Halliday, D., and Curtis, A. [2010] An interferometric theory of source-receiver scattering and imaging. Geophysics, **75**, SA95–SA103.

Ravasi, M. and Curtis, A. [2013] Nonlinear scattering based imaging in elastic media: theory, theorems and imaging conditions. Geophysics, **78**, (3).

Stolt, R. and Weglein, A. [1985] Migration and inversion of seismic data. Geophysics, **50**, 2458-2472.

Vasconcelos, I. [2013] Source-receiver reverse-time imaging of dual-source, vector-acoustic seismic data. Geophysics, **78**, (2), WA147-WA158.

Vasconcelos, I., Sava, P., and Douma, H. [2010] Nonlinear extended images via image-domain interferometry. Geophysics, **75**, (6), SA105–SA115.

Wapenaar, K., Broggini, F., Slob, E., and Snieder, R. [2013] Three-Dimensional Single-Sided Marchenko Inverse Scattering, Data-Driven Focusing, Green's Function Retrieval, and Their Mutual Relations. Physical Review Letters, **110**, (8), 084301.